

Up-regulation of Tumor Susceptibility Gene 101 Protein in Ovarian Carcinomas Revealed by Proteomics Analyses*

Travis W. Young[‡], Fang C. Mei[‡], Daniel G. Rosen[§], Gong Yang[§], Nan Li[‡], Jinsong Liu^{§¶}, and Xiaodong Cheng^{‡||}

Small GTPase RAS plays a critical role in cellular signaling and oncogenic transformation. Proteomics analysis of genetically defined human ovarian cancer models identified the tumor susceptibility gene 101 (TSG101) as a downstream target of RAS oncogene. Mechanistic studies revealed a novel post-translational regulation of TSG101 through the RAS/RAF/MEK/MAPK signaling pathway and downstream molecules p14^{ARF}/HDM2. Immunoblot analysis using ovarian cancer samples and microtissue array revealed elevated TSG101 levels in human ovarian carcinomas. Silencing of TSG101 by short interfering RNA in ovarian cancer cells led to growth inhibition and cell death. Concurrent with the apparent growth-inhibitory effect, the levels of the CBP/p300-interacting transactivator with ED-rich tail 2 (CITED2) and hypoxia-inducible factor 1 α (HIF-1 α), as well as its cellular activity, were markedly reduced after TSG101 knockdown. These results demonstrate that TSG101 is important for CITED2- and HIF-1 α -mediated cellular regulation in ovarian carcinomas. *Molecular & Cellular Proteomics* 6:294–304, 2007.

Oncogenic transformation is an intricate process involving alterations of multiple genetic elements and signaling cascades. One critical signaling molecule that contributes directly to transformation is the small G-protein RAS. Activation of the K-RAS or H-RAS signaling pathways plays an important role in ovarian tumorigenesis. Mutations in K-RAS and its downstream effector B-RAF are involved in 60–70% of low grade serous ovarian cancers (1, 2). Although activating mutations of H-RAS are present in only about 6% of ovarian cancers (3), activation of H-RAS upstream and downstream effector pathways often occurs in the absence of an H-RAS mutation (4). For example, the upstream signaling molecule Her-2/Neu and the immediate downstream RAS effector B-RAF are found to be up-regulated and active in a large portion of ovarian cancers (5, 6).

From the [‡]Department of Pharmacology and Toxicology, Sealy Center for Cancer Cell Biology, School of Medicine, The University of Texas Medical Branch, Galveston, Texas 77555 and [§]Department of Pathology, The University of Texas M. D. Anderson Cancer Center, Houston, Texas 77030

Received, August 10, 2006, and in revised form, October 30, 2006
Published, MCP Papers in Press, November 16, 2006, DOI 10.1074/mcp.M600305-MCP200

RAS functions as an intracellular molecular switch, cycling between the GDP-bound inactive state and the GTP-bound active state in response to external stimuli leading from cell surface receptor tyrosine kinases to nuclear transcription factors (7, 8). RAS-associated cell signaling is involved in many important cellular processes, such as cell growth, differentiation, and survival under physiological conditions. Several well known intracellular signaling cascades including the RAF/MEK¹/ERK pathway, the phosphatidylinositol 3-kinase pathway, and the RAL-guanine nucleotide dissociation stimulator pathway have been identified as mediators of RAS downstream effects (9–14). At the present time the precise molecular mechanism of RAS-mediated oncogenic transformation is not clear. Particularly how oncogenic RAS mutants, in collaboration with other oncogenes and tumor suppressors, perturb the balance of cellular signaling networks and lead to the formation of cancer cells remains undefined.

One particular protein implicated in tumorigenic processes that has garnered significant interest in recent years is the tumor susceptibility gene 101 (TSG101). TSG101 was originally identified as a potential tumor suppressor from a controlled homozygous functional knock-out screen. Inactivation of TSG101 in NIH3T3 mouse fibroblasts leads to focus formation in monolayer cell cultures, anchorage-independent growth in soft agar, and *in vivo* tumor formation in nude mice (15). Initial studies suggested that TSG101 was often mutated in human breast cancers (16), and its aberrant splice variants were frequently detected in different tumor types (17–22). However, it was subsequently determined that these apparent mutations were in fact alternative splice variants generated exclusively by exon skipping (23).

¹ The abbreviations used are: MEK, mitogen-activated protein kinase/extracellular signal-regulated kinase kinase; 2-DE, two-dimensional electrophoresis; CITED2, CBP/p300-interacting transactivator with ED-rich tail 2; GFP, green fluorescent protein; HMD2, human homolog of MDM2; HIF, hypoxia-inducible factor; MDM2, mouse double minute 2; MTT, 3-(4,5-dimethylthiazol-2-yl)-2,5-diphenyl tetrazolium bromide; TSG101, tumor susceptibility gene 101; siRNA, short interfering RNA; MAPK, mitogen-activated protein kinase; CBP, cAMP-response element-binding protein (CREB)-binding protein; ERK, extracellular signal-regulated kinase; PI3K, phosphatidylinositol 3-kinase; Tricine, N-[2-hydroxy-1,1-bis(hydroxymethyl)ethyl]glycine; HRE, HIF-1 α response element.

Although TSG101 is essential for cell proliferation, cell survival, and embryonic development under normal physiological conditions (24–27), the role of TSG101 in tumor formation and development has proven to be complex and remains controversial. TSG101 was initially described as a potential tumor suppressor, and the expression of TSG101 has been shown to be decreased in certain cancer samples (28). However, more recent studies suggest that TSG101 levels are elevated in human cancers, including thyroid (29) and gastrointestinal tumors (30). Furthermore overexpression of TSG101 can also lead to neoplastic transformation (15). Gene silencing of TSG101 leads to growth arrest and cell death in breast and prostate cancer cells (31) instead of growth promotion as would be expected for the loss of a true tumor suppressor. We propose that TSG101 is an important factor for maintaining normal cellular homeostasis and that elevated TSG101 expression contributes to oncogenic transformation. This hypothesis is consistent with the fact that steady-state TSG101 levels are tightly controlled in normal cells, primarily at the post-translational level, keeping protein concentrations within a narrow range (32). At the present time, the mechanism of TSG101 post-translational regulation is not clear. Understanding the cellular regulation of TSG101 is important for further elucidating the function of TSG101 under physiological and neoplastic conditions.

In this study, we identified TSG101 as a RAS downstream target in human ovarian epithelial cells transformed by either oncogenic *H-RAS*^{V12} or *K-RAS*^{V12} using a two-dimensional electrophoresis (2-DE)-based proteomics analysis. Immunohistochemical analysis of ovarian cancer tissue array revealed that TSG101 is up-regulated in more than 70% of human ovarian carcinomas. Gene silencing using TSG101-specific siRNA inhibited the growth and tumorigenicity of SKOV-3 cells, a naturally occurring ovarian cancer cell line with elevated RAS activity. Our study for the first time provides a direct link between oncogenic RAS and TSG101 and demonstrates a potential role for TSG101 in RAS-mediated oncogenic transformation through regulation of the CBP/p300-interacting transactivator with ED-rich tail 2 (CITED2) and hypoxia-inducible factor 1 α (HIF-1 α).

MATERIALS AND METHODS

Cell Culture—T29, T29H, and T29K cells were generated through retroviral transfection as described previously (33) and grown in Medium 199/MCDB105 medium (1:1) (Sigma) containing 10% fetal bovine serum and 1% penicillin/streptomycin (Invitrogen). SKOV-3 cells were maintained in RPMI 1640 medium containing 5% fetal bovine serum (Invitrogen) and 1% penicillin/streptomycin (Invitrogen).

2-DE Analysis—2-DE proteomics analysis was performed as described previously (34, 35). Briefly cells were trypsinized, washed in PBS, and lysed in buffer containing the following: 7 M urea, 2 M thiourea, 4% CHAPS, 1 mM EDTA, 1 mM EGTA, 60 mM DTT, 1 mM PMSF, 25 μ g/ml leupeptin, 10 μ g/ml aprotinin, 1 mM benzamidine, 1 mM sodium orthovanadate, and 1 mM microcystin. Total protein concentration was determined using the Bradford assay (Bio-Rad), and 500 μ g was loaded onto 18-cm Immobiline pH gradient strips (GE

Healthcare). After focusing for 56,000 V-h, strips were loaded onto 10% SDS-Tricine gels and electrophoresed for 20 h at 140 V. Gels for analysis and for protein excision were stained with silver as described previously (36, 37). Images were analyzed using Phoretix 2-D software (Nonlinear Dynamics). Spots of interest were excised and in-gel digested with trypsin as described previously (34). Proteins were identified by MALDI-TOF analysis by comparison of tryptic fragment profiles with the National Center for Biotechnology Information (NCBI) database for theoretical peptide cleavage patterns.

Immunoblotting Analysis—The protein concentration of cell lysates was assayed with the Bio-Rad protein assay reagent. Equal amounts of protein were loaded onto 12% SDS-polyacrylamide minigels (Bio-Rad) or 10% Tricine-SDS gels and transferred to PVDF membranes. PVDF blots and the remaining polyacrylamide gels were stained with Ponceau S and Coomassie Blue, respectively, to ensure equal loading and even transfer of the samples. After being blocked overnight in 5% milk in TBS-Tween, blots were incubated with corresponding primary antibodies for 1.5 h followed by horseradish peroxidase-conjugated secondary antibody (1:4000, Bio-Rad) for 45 min. Antigen-antibody complexes were detected by enhanced chemiluminescence (Pierce).

Gene Expression Analysis—Total RNA was isolated from cells using TRIzol reagent (Invitrogen), and the concentration was determined by absorbance at 260 nm. Real time PCR analysis was carried out using fluorescent TSG101 primers on an Applied Biosystems Prism 7000 sequence detection system. RT-PCR was carried out for TSG101 and HIF-1 α using 1 μ g of isolated total RNA under the following parameters: 94 °C for 1 min, 57 °C for 1 min, and 72 °C for 1.5 min; 35 cycles. Primers used for RT-PCR were TSG101 forward (5'-TCCAGTCTTCTCTCGTCCTATTTC-3') and reverse (5'-TTTCTCC TTCATCCGCCATCTC-3') and HIF-1 α forward (5'-CCTGCACTCAATCAAGAATTGC-3') and reverse (5'-TTCTGCTCTGTTTGGTGAGGCT-3').

RAS Pathway Inhibitor Studies—For chemical inhibitor experiments, cells were grown to 50–60% confluence in 6-well plates and treated with DMSO vehicle or the following for 24 h: 20 μ M U0126 (MEK inhibitor), 10 μ M LY294002 (PI3K inhibitor), or 10 μ M FTI-277 (H-RAS farnesylation inhibitor). Following treatments, cells were lysed, and the levels of total and cytoplasmic TSG101 were examined by immunoblotting using specific anti-TSG101 antibody (1:1000, Novus).

Inhibition of H-RAS Gene Expression by Retroviral siRNA—SKOV-3 and T29H cells were transfected with two retrovirus-mediated *H-RAS* siRNA vectors (designated H1 and H2) that have been described previously (38). Briefly H1 selectively silences mutant *H-RAS*^{V12}, whereas H2 suppresses both the *H-RAS*^{V12} mutant and wild-type *H-RAS* expression. SKOV-3 and T29H cells grown to 50% confluence in 10-cm plates were transfected with H1 and H2 retroviral supernatants generated from Phoenix viral packaging cells. Following transfection, cells were selected for 7–10 days in 0.7 mg/ml G418 to establish stable cell lines. RAS-GTP binding assays and Western blotting using anti-H-RAS (1:2000, Santa Cruz Biotechnology) were used to measure the expression and activation levels of RAS proteins in these siRNA cell lines.

Immunohistochemical Analysis—The tissue microarray slides were subjected to immunohistochemical staining as follows. After initial deparaffinization, endogenous peroxidase activity was blocked using 0.3% hydrogen peroxide. Deparaffinized sections were microwaved in 10 mM citrate buffer (pH 6.0) to unmask the epitopes. The slides were then incubated at 4 °C overnight against TSG101 (1:100, Clone 4A10, Novus Biologicals), next with biotin-labeled secondary antibody for 20 min, and finally with a 1:40 solution of streptavidin: peroxidase for 20 min. Tissues were then stained for 5 min with 0.05% 3',3'-diaminobenzidine tetrahydrochloride that had been

freshly prepared in 0.05 M Tris buffer at pH 7.6 containing 0.024% H₂O₂, then counterstained with hematoxylin, dehydrated, and mounted. All of the dilutions of antibody, biotin-labeled secondary antibody, and streptavidin-peroxidase were made in phosphate-buffered saline (pH 7.4) containing 1% bovine serum albumin. Negative controls were made by replacing the primary antibody with phosphate-buffered saline. All controls gave satisfactory results. Immunostaining for TSG101 was analyzed by computerized automated image analysis (Ariol SL-50, Applied Imaging, San Jose, CA). Quantitation was done on the whole core tissue at 20 \times considering only tumor epithelial cells by appropriate training of the computerized system. Immunostaining for TSG101 was measured as the total integrated optical density and expressed in arbitrary optical density units (Σ OD). These units are expressed in a range from 0 to 255. An optical density unit closer to 0 corresponds to darker pixels, whereas a value closer to 255 corresponds to lighter pixels. Therefore, a Σ OD low value translates as a higher expression, and a high Σ OD value translates as a lower expression for the marker. For statistical analysis, all cases displaying total integrated optical density (mean \pm S.E.) were then grouped together on a 0–3 scale. Negative staining (score 0) was defined as the total absence of marker (brown color). The mean of the results from the two replicate core samples from each tumor specimen was considered for each case. Counting criteria and software settings were identical for all slides. Quantitation was done blinded to clinicopathologic information. Normal ovarian epithelial cells were used as a comparison for intensity and pattern of staining.

Overexpression of HDM2 in T29H and SKOV-3 Cells—Freshly plated T29H cells (2×10^5 cells/plate in 6-cm plates) and SKOV-3 cells at 80% confluence were transfected with HDM2 vector (1 μ g) using Lipofectamine 2000 (Invitrogen) according to the manufacturer's instructions. Cells were harvested at 24 and 48 h post-transfection or further selected for the generation of stable lines using 0.7 mg/ml G418. Whole cell lysates were processed as described above, and Western blots were probed using anti-HDM2 (1:1000, Santa Cruz Biotechnology).

Transfection of SKOV-3 Cells with siRNA and HIF-1 α Green Fluorescent Protein (GFP) Reporter—Cells were plated at 1×10^5 in 3.5-cm wells and grown overnight at 37 $^{\circ}$ C. The following day cells were transfected with either control siRNA duplex or TSG101 siRNA duplex at 375 ng/well (Dharmacon) using Lipofectamine 2000. Cells were then passaged at 48 h post-transfection and used for subsequent experiments. The HIF-1 α response element (HRE)-GFP reporter (a generous gift from Mark Dewhirst) was transfected into cells 48 h after transfection with siRNA reagents, and cells were subsequently plated onto microscope coverslips. On the 5th day following siRNA transfection, cells on coverslips were rinsed in PBS and fixed in 2% paraformaldehyde for 15 min. Nuclear staining was carried out with 4',6-diamidino-2-phenylindole (5 ng/ml) for 5 min after which slides were mounted and observed using a fluorescence microscope (Olympus BX51) equipped with a Hamamatsu digital camera (C4742-95).

Cell Growth and Viability Assays—SKOV-3 cells were trypsinized 48 h post-transfection with siRNAs and plated at 2×10^3 cells/well in 96-well plates with five wells for each treatment. On subsequent days, medium was removed, and 100 μ l/well fresh medium was added along with 10 μ l of 3-(4,5-dimethylthiazol-2-yl)-2,5-diphenyl tetrazolium bromide (MTT) to a final concentration of 500 μ g/ml. Cells were incubated for 3 h at 37 $^{\circ}$ C and then lysed by adding 200 μ l/well DMSO and incubating at 37 $^{\circ}$ C for 1 h. Cell viability was measured by reduction of MTT, which registered absorbance at 595 nm on a Molecular Devices microplate reader.

In Vivo Tumor Growth Assays—SKOV-3 cells were trypsinized 3 days following transfection with either control or TSG101 siRNA and subsequently washed and resuspended in phosphate-buffered saline

at 5×10^6 cells/ml. 200 μ l (1×10^6 cells) of control or TSG101-transfected cells were injected subcutaneously into the right and left flanks (respectively) of 4–6-week-old BALB/c athymic nude mice (The Jackson Laboratory, Bar Harbor, ME). Mice were examined every 5 days until visible tumors appeared. Subsequently tumor volume measurements were taken every 3–5 days, mice were sacrificed 6 weeks after initial injections, and a final measurement of tumor volume was taken.

RESULTS

Identification of Protein Targets Associated with H-RAS and K-RAS-mediated Oncogenic Transformation by 2-DE-based Proteomics—To systematically investigate the molecular mechanisms of oncogene RAS-mediated transformation and to explore the important signaling events associated with transformation of human ovarian epithelial cells, we compared the total protein expression profiles of three genetically engineered cell lines, T29, T29H, and T29K, derived from human ovarian surface epithelial cells. Although T29 cells stably transfected with SV40 T/t antigens and human telomerase reverse transcriptase are fully immortalized, only the addition of oncogenic H-RAS (in T29H) or K-RAS (in T29K) leads to the malignant transformation of T29 cells (33). To eliminate clonal variability, pools of early passages of T29, T29H, and T29K were used in this study. Total cell lysates from each cell line were analyzed by 2-DE using Immobiline dry strips (pH 4–7) and 10% Tricine-SDS-polyacrylamide gels. For each cell line, at least two independent cell lysates were prepared from cultures at different early passages, and four or more well resolved gels from six different runs were analyzed.

Fig. 1 shows representative silver-stained 2-DE images of T29, T29H, and T29K. Approximately 2200 distinct protein spots were resolved within each gel. The intensity of each protein spot was determined, normalized to the sum of intensities of all spots on the gel, and quantified as a percentage of volume in each gel using Phoretix 2-D analysis software (Non-linear Dynamics). Each individual protein spot was then matched with the identical protein spot from each replicate gel. Data for these matched spots were then averaged over replicate gels for each cell line. The average normalized volume of each spot in the transformed T29H or T29K cells was then compared with that of the matched spot in immortalized T29 cells. To determine what would constitute significant changes between transformed and untransformed cells, the intrinsic variance of each protein spot was determined for each cell line. The average variance for individual spots in the replicate gels for the T29, T29H, and T29K were 34, 29, and 30%, respectively. Based on these observed values, we selected spots whose average normalized volume increased or decreased by at least 1.5-fold between the T29 and T29H/T29K cell lines as significantly changed candidates. A total of 143 protein spots were identified to differ significantly between T29 and T29H cells, whereas 117 protein spots were changed significantly between T29 and T29K cells. Interestingly of these altered spots, only about 40 spots are common

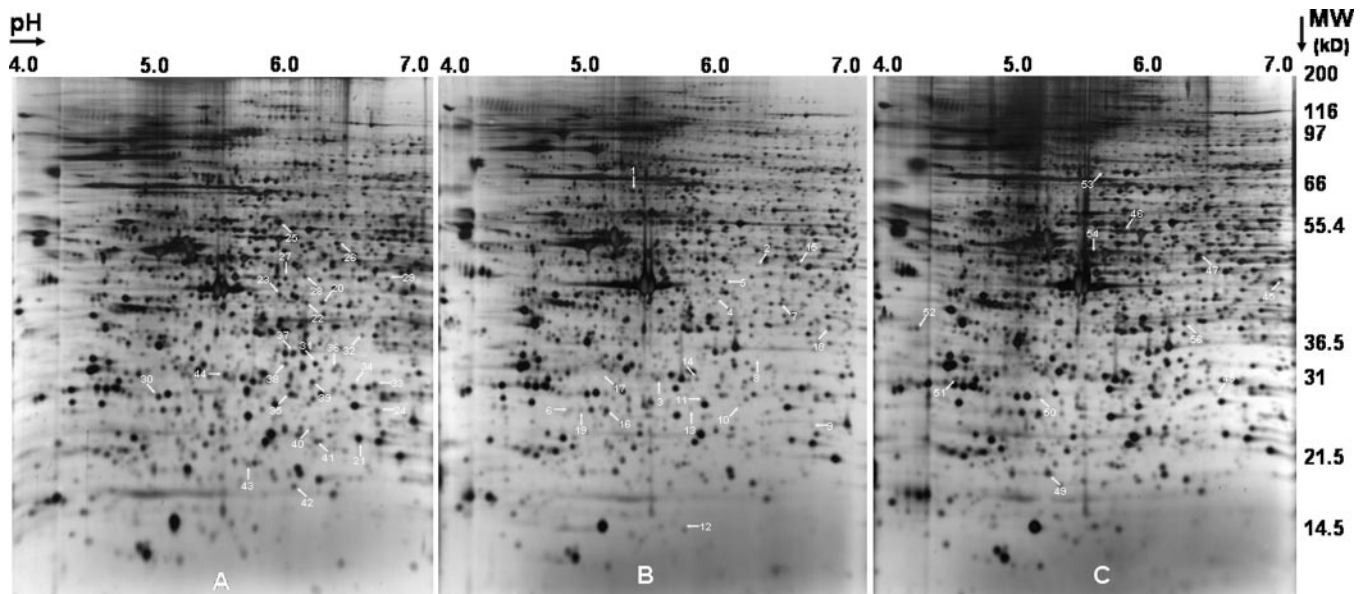


FIG. 1. **Proteomics analysis of T29, T29H, and T29K cells using 2-DE gels.** Whole cell lysates (200 μ g) from T29H (A), T29 (B), and T29K (C) cells were separated on a 2-DE gel and visualized by silver staining. *Arrows* indicate identified protein spots significantly altered between T29 and T29H cells (A) or between T29 and T29K cells (C) as well as protein spots significantly altered in both T29H and T29K cells when compared with T29 cells (B).

between T29H and T29K. Using peptide mass fingerprinting, we successfully identified 55 of these altered protein spots (Table I). The apparent observed molecular mass and pI for all identified proteins matched very well with their calculated values.

Up-regulation of TSG101 in *RAS*^{V12}-transformed Human Ovarian Epithelial Cells—TSG101 was identified as a protein that was up-regulated in both the *K-RAS*^{V12}- and *H-RAS*^{V12}-transformed ovarian epithelial cell line (Fig. 2, A and B). The protein level of TSG101 was up-regulated ~2-fold in T29H and T29K cells as compared with its immortalized counterpart, T29 cells. This up-regulation was further confirmed by immunoblotting analysis of total protein lysates from T29 and T29H cells using an antibody specific to TSG101 (Fig. 2C). To check whether the apparent increase in TSG101 protein was due to the transcriptional regulation of the TSG101 gene, the levels of TSG101 mRNA in T29 and T29H cells were examined by semiquantitative (Fig. 2D) and real time PCR (Fig. 2E). Both methods showed no significant change in TSG101 mRNA levels between T29 and T29H cells, indicating that the regulation of TSG101 occurs at the post-transcriptional level in *H-RAS*^{V12}-transformed human ovarian epithelial cells. This is consistent with an earlier mRNA expression array study showing that the transcription levels of TSG101 were not significantly different in T29 and T29H cells (33).

Regulation of TSG101 by *RAF/MEK/MAPK* Pathway—To further determine whether the change in TSG101 levels is a direct effect of elevated RAS activity in T29H cells, we examined the TSG101 protein levels in response to FTI-277, a pharmacological inhibitor that represses H-RAS activation

through inhibiting the farnesylation of H-RAS (39). As shown in Fig. 3A, FTI-277 caused a significant decrease of TSG101 in T29H cells, suggesting that TSG101 up-regulation was directly linked to the level of H-RAS activation. Due to the fact that FTI-277 is a general farnesyltransferase inhibitor and could cause cellular effects other than H-RAS inhibition, we used a retrovirus-based siRNA technique to specifically inhibit H-RAS activity. Although H1 siRNA inhibits oncogenic H-RAS^{V12} specifically, the H2 siRNA vector suppresses both endogenous wild-type and oncogenic H-RAS. The specificity and effectiveness of H1 and H2 siRNAs have been demonstrated in our previous publications (34, 38). Stable expression of H1 and H2 in T29H cells led to significant reduction in the levels of TSG101 protein (Fig. 3B) accompanied with decreased RAS protein levels and activities (data not shown), confirming that H-RAS is indeed directly responsible for the up-regulation of TSG101 in this cell line.

To dissect the cellular signaling mechanism by which H-RAS impinges on TSG101 regulation, we used inhibitors for known RAS effector pathways. The MEK inhibitor U0126 significantly decreased cellular TSG101 to levels similar to that of untransformed T29 cells and cells treated with FTI-277, whereas the phosphatidylinositol 3-kinase inhibitor LY294002 showed minimal effects on TSG101 levels (Fig. 3A). These results indicate that oncogenic H-RAS^{V12}, signaling through MEK but not PI3K kinase, up-regulates TSG101 post-transcriptionally.

To ensure that H-RAS-mediated post-transcriptional regulation of TSG101 does not just occur in the genetically defined T29H human ovarian cancer cell model, we examined the effect of altering H-RAS activity on modulation of TSG101 in a naturally derived ovarian cancer cell line, SKOV-3. This cell

TABLE I

Proteins identified by mass spectrometry to be changed significantly between T29 and T29H/T29K cells

The spot numbers correspond to those on the master images in Fig. 1. NP, spot not present; MW, molecular weight; Obs, observed; THO, TEX1 homolog; PEF, Penta-EF hand containing protein; SPFH, stomatins, prohibitins, flotillins, HfLK/C.

Spot no.	Protein ID	NCBI accession no.	MW	pI	MW _{Obs}	pI _{Obs}	-Fold change	
							H-RAS	K-RAS
Proteins commonly changed								
1	L-plastin variant	BAD92221	56.2	5.2	67	5.2	-6.43	NP
2	Caspase 4 isoform α precursor	NP_001216	43.3	5.7	49	6.0	4.12	1.66
3	Cathepsin D preproprotein	NP_001900	44.6	6.1	31	5.4	-2.96	-2.39
4	Calponin 3	NP_001830	36.4	5.7	40	5.8	2.54	2.73
5	Selenophosphate synthetase	NP_036397	42.9	5.6	44	5.9	1.55	1.52
6	Human glyoxalase I	1Q1P	20.9	5.1	26	4.8	2.82	2.8
7	Gelsolin-like capping protein	NP_001738	38.5	5.9	40	6.3	1.68	1.63
8	Nicotinate-nucleotide pyrophosphorylase	Q15274	31.1	5.8	34	6.1	16.13	9.21
9	Peroxiredoxin 3 isoform b	NP_054817	26.1	7.1	23	6.4	7.04	2.71
10	Guanidinoacetate <i>N</i> -methyltransferase isoform a	NP_000147	26.3	5.7	26	5.9	3.9	1.85
11	NADH dehydrogenase ubiquinone	NP_004542	30.2	7	27	6.0	2.2	1.54
12	Phosphohistidine phosphatase I	NP_054891	13.8	5.7	13	5.5	2.03	2.22
13	Phosphoserine phosphatase	NP_004568	25.0	5.5	25	5.5	7.34	3.75
14	Latexin	AAH05346	25.8	5.5	30	5.6	2.34	2.45
15	Tumor susceptibility gene 101	NP_006283	43.9	6.1	45	6.2	1.83	2.04
16	Glyoxalase I	NP_006699	20.7	5.2	25	5.0	2.03	2.33
17	Calretinin (calbindin 2)	NP_001731	31.5	5.1	32	5.0	NP	-3.25
18	Serine/threonine phosphatase 1 γ	BAA82664	34.5	5.1	32	6.6	-1.56	-2.07
19	<i>Homo sapiens</i> 14q32 jagged gene	AAD15563	31.9	5.9	26	4.9	1.97	2.58
Proteins solely changed in T29H								
20	Calponin 3	NP_001830	36.4	5.7	40	6.1	2.09	1.44
21	Peroxiredoxin 3	NP_006784	27.7	7.7	25	6.4	1.72	1.14
22	THO complex 3 (THOC3)	NP_115737	39.4	5.7	35	6.0	1.5	1.28
23	SPFH domain family, member 2 isoform 1	NP_009106	37.8	5.5	42	5.6	1.71	1.33
24	Protein-L-isoaspartate O-methyltransferase	NP_005380	24.6	6.7	26	6.5	1.99	1.41
25	Copine I	NP_003906	59.2	5.5	60	5.7	-2.76	-1.12
26	Aldehyde dehydrogenase, mitochondrial precursor	P05091	56.4	7	55	6.1	1.54	1.18
27	Mannose-6-phosphate isomerase	NP_002426	46.6	5.6	46	5.8	1.62	1.02
28	CGI-17 protein	AAH22789	43.8	5.9	40	6.0	2.15	1.31
29	Ornithine aminotransferase, mitochondrial precursor	P04181	48.5	6.6	47	6.5	-1.66	1.25
30	Calpain, small subunit I	NP_001740	28.3	5.1	28	4.9	-1.54	-1.12
31	3-Hydroxyisobutyrate dehydrogenase	NP_689953	32	5.8	35	5.8	1.60	1.33
32	Aminoacidipate-semialdehyde dehydrogenase-phosphopantetheinyl transferase	NP_056238	35.8	6.4	38	6.4	1.89	-1.38
33	Δ^3, Δ^2 -Enoyl-CoA isomerase	AAA35485	29.4	6.4	30	6.5	1.73	1.05
34	Mitochondrial short-chain enoyl-CoA hydratase 1 precursor	NP_004083	31.4	8.3	29	6.3	1.67	1.05
35	Thioredoxin peroxidase	NP_006397	30.5	5.9	28	5.9	1.50	1.38
36	PEF	AAQ89370	30.6	6.1	28	6.2	1.54	-1.22
37	Replication protein A2, 32 kDa	NP_002937	29.2	5.8	32	6.0	2.08	-1.05
38	S phase protein	AAQ97193	29.9	5.7	28	5.8	2.04	1.24
39	6-Phosphogluconolactonase	NP_036220	27.5	5.7	30	6.0	1.59	1.18
40	DNA-directed RNA polymerase II polypeptide E	NP_002686	24.7	5.7	25	6.0	2.51	1.09
41	Chain A, human Dj-1 with sulfinic acid	1SOAA	20	6.3	25	6.1	1.7	-1.05
42	Mago-Nashi homolog	NP_002361	17.1	5.7	16	5.9	4.77	-1.26
43a	Membrane type 1 matrix metalloproteinase cytoplasmic tail-binding protein-1	NP_060739	21.5	5.4	18	5.5	-2.18	-1.26
43b	Stathmin	NP_005554	17.3	5.8	18	5.5	-2.18	-1.26
44	Cathepsin D preproprotein	NP_001900	44.6	6.1	30	5.3	2.08	1.29
Proteins solely changed in T29K								
45	Methionine adenosyltransferase II, α	NP_005902	43.6	6	44	6.8	1.53	-3.09
46	Vimentin	NP_003371	53.7	5.1	50	5.7	1.42	2.22
47	Calcium-binding transporter	AAF28888	46.1	5.3	45	6.3	-1.28	-2.01
48	Similar to GrpE protein homolog 1, mitochondrial precursor	XP_052625	19.7	6.2	27	6.3	1.17	-2.75
49	Eukaryotic translation initiation factor 5A	NP_001961	17	5.1	24	5.2	1.24	-2.57
50	Rho GDP dissociation inhibitor (GDI) α	NP_004300	23.3	5	27	5.1	1.23	-2.07
51	14.3.3 protein	AAC28640	19.9	4.5	27	4.5	1.05	-2.59
52	Clathrin, light polypeptide A, isoform a	NP_001824	23.6	4.5	31	4.3	1.26	-3.87
53	Keratin 1	NP_006112	66.2	8.2	78	5.5	1.18	1.68
54	Cytokeratin 18	CAA31377	47.3	5.3	44	5.4	1.22	2.53
55	Isocitrate dehydrogenase 3 (NAD ⁺) α precursor	NP_005521	40	6.7	32	6.1	-1.01	-1.7

Downloaded from www.mcponline.org at UNIV OF TEXAS MEDICAL BRANCH on August 3, 2007



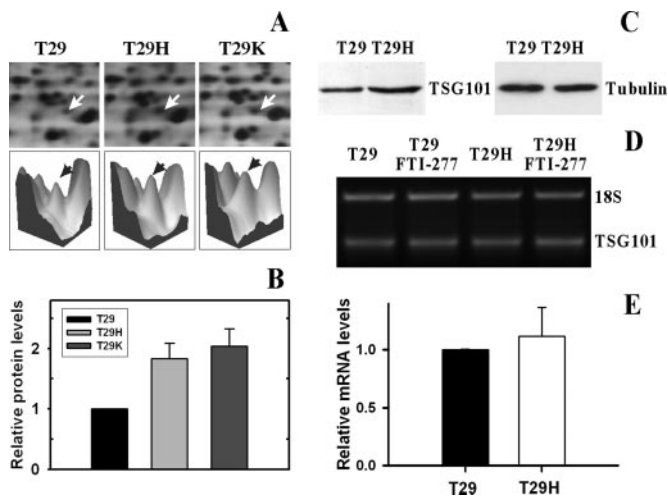


FIG. 2. Post-transcriptional regulation of TSG101 in RAS-transformed cells. *A*, protein levels of TSG101 in T29, T29H, and T29K cells revealed by 2-DE gel analysis. *Arrows* denote spot identified as TSG101. *B*, quantitative measurement of TSG101 protein levels in T29, T29H, and T29K cells ($n = 4$). *C*, protein levels of TSG101 in T29H and T29 cells revealed by immunoblotting analysis using TSG101-specific antibodies. *D*, mRNA levels of TSG101 in T29 and T29H cells in the presence and absence of the H-RAS inhibitor FTI-277 measured by semiquantitative reverse transcription-PCR. *E*, comparison of TSG101 mRNA expression levels in T29 and T29H cells as determined by real time PCR analysis from multiple independent purified RNA samples ($n = 3$).

line does not contain an oncogenic RAS allele, but nonetheless exhibits elevated levels of RAS activity (38). TSG101 protein levels in SKOV-3 cells, which are expressed at levels similar to those in T29H cells, showed a marked decrease following specific gene silencing of endogenous RAS with H2 siRNA specific for wild-type H-RAS (Fig. 3C), whereas H1 siRNA specific for oncogenic H-RAS^{V12} had no effect. These data suggest that the regulatory effect of H-RAS signaling on TSG101 is present not only in T29H cells but also in other naturally derived human ovarian cancer cells.

H-RAS Regulates TSG101 through p14^{ARF}/HDM2—After ascertaining the connection between oncogene RAS activity and the cellular levels of TSG101, it is imperative to establish the molecular mechanism by which H-RAS post-transcriptionally regulates TSG101. It has been suggested that the oncoprotein MDM2 (HDM2 in humans) can regulate the cellular level of TSG101 through a negative feedback loop (40), and because it has been well established that RAS can exert opposing effects on MDM2 (induction of MDM2 transcription and conversely activation of the MDM2 inhibitor p14^{ARF} via the RAF/MEK/MAPK pathway) (41), we hypothesized that H-RAS might regulate TSG101 levels through modulation of p14^{ARF} and HDM2. Consistent with this hypothesis, we found that oncogenic RAS up-regulated p14^{ARF} in T29H cells, and this increased cellular level of p14^{ARF} can be suppressed by U0126, a specific inhibitor of the RAS downstream target MEK (Fig. 4A). Up-regulation of p14^{ARF} by RAS sequestered

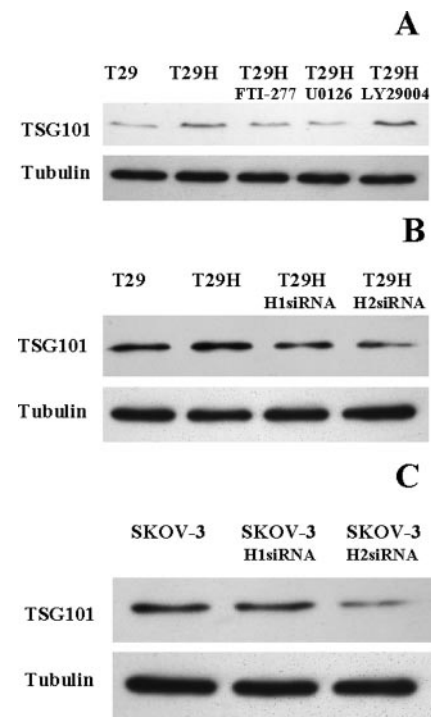


FIG. 3. TSG101 up-regulation is H-RAS-specific and mediated through the MEK/ERK cell signaling pathway. *A*, cells were pre-treated for 24 h with FTI-277 (H-RAS inhibitor), U0126 (MEK-specific inhibitor), and LY294002 (PI3K-specific inhibitor). Equivalent amounts of cellular lysates were separated by 12% SDS-PAGE, transferred to PVDF membranes, and probed with TSG101 antibody. *B*, cells were stably transfected with retroviral siRNA constructs against either H-RAS^{V12} only (H1) or both wild-type and oncogenic RAS (H2). Cell lysates on PVDF membranes were probed with TSG101 antibody. Equal protein loading was determined by Ponceau S staining of PVDF membranes. *C*, SKOV-3 cells were transfected with H1 and H2 siRNA. Cell lysates were harvested, separated by 12% SDS-PAGE, transferred to PVDF membranes, and probed with TSG101 antibody. Gel images are representative of three independent experiments.

HDM2 in the nucleus and led to a reduction of cytoplasmic HDM2 levels in T29H cells despite the fact that the total cellular levels of HDM2 were up-regulated in T29H cells (Fig. 4B). The cytoplasmic levels of HDM2 were restored in cells where H-RAS^{V12} levels were suppressed by H1 and H2 siRNA vectors (Fig. 4B), suggesting that oncogenic RAS activity is directly responsible for the reduction of cytoplasmic HDM2. To test whether decreased cytoplasmic HDM2 levels in T29H cells are indeed liable for the up-regulation of TSG101 through a negative regulatory loop as suggested, we monitored the levels of cellular TSG101 in T29H cells in response to ectopic overexpression of HDM2. As shown in Fig. 4C, overexpression of HDM2 in T29H led to a significant decrease in TSG101 protein levels. Similar results were observed in SKOV-3 cells. Taken together, these data suggest that oncogenic RAS activates the HDM2 inhibitor p14^{ARF} through the RAF/MEK/MAPK signaling pathway, suppressing cellular HDM2 activity and consequently resulting in an increase in overall cellular levels of TSG101.

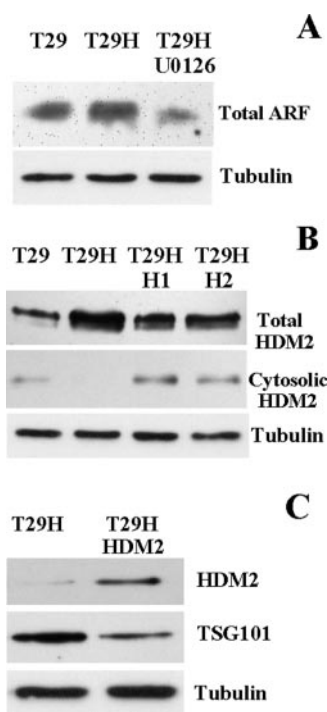


FIG. 4. Dependence of RAS-mediated TSG101 modulation on p14ARF/HDM2. A, total cellular levels of p14ARF in T29 and T29H cells were determined by immunoblotting using p14^{ARF}-specific antibody. B, total and cytoplasmic levels of TSG101 from T29 cells compared with those of T29H cells and T29H cells stably transfected with H1 and H2 retroviral siRNAs as described under "Materials and Methods." C, total protein levels of HDM2 and TSG101 from T29H cells and T29H cells stably expressing ectopic HDM2. Similar results were obtained from two independent experiments.

Up-regulation of TSG101 in Human Ovarian Cancer Samples—To investigate the clinical association of RAS-mediated TSG101 up-regulation in human ovarian surface epithelial cells, we compared the expression levels of TSG101 in normal human ovarian and ovarian cancer samples using an affinity-purified mouse anti-human TSG101 monoclonal antibody (Clone 4A10) by immunoblotting analysis. Although normal ovarian tissue lysates did not show significant expression for TSG101, the expression of TSG101 was increasingly positive in low grade and high grade carcinomas (Fig. 5). To further confirm the clinical association of RAS-mediated TSG101 up-regulation in human ovarian surface epithelial cells, we probed the expression levels of TSG101 in ovarian carcinomas using human ovarian cancer tissue arrays. The relative optical density of the marker expression was measured and then analyzed using a non-parametric test. Again an increased expression in TSG101 levels in ovarian tumors (ΣOD , 68 ± 16) was observed as compared with those of normal ovarian surface epithelial cells (ΣOD , 102 ± 15). Although the levels varied from negative (26.3%) to strongly positive (23%) among 152 primary ovarian carcinoma samples analyzed (Table II), the increased TSG101 expression observed in ovarian

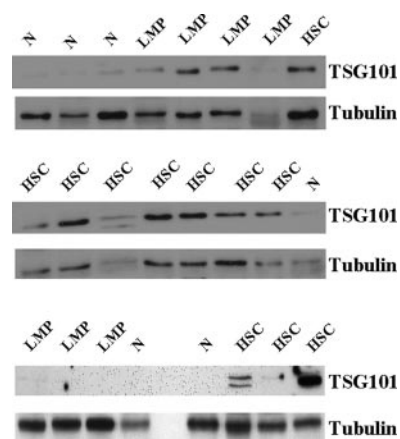


FIG. 5. Expression levels of TSG101 in human ovarian cancers. Immunoblotting analysis showed negative to weak expression for TSG101 in normal human ovarian tissue (N), weak to medium expression in low malignant potential ovarian tumors (LMP), and strong positive expression in high grade serous carcinomas (HSC).

TABLE II
Expression levels of TSG101 in human ovarian carcinomas

Score	Number of cases	Percentage of total cases
0	40	26.3
1	37	24.4
2	40	26.3
3	35	23
Total	152	100

tumors is statistically significant (Kruskal-Wallis analysis of variance: χ^2 , 86.74; $p < 0.0001$).

TSG101 Is Required for Growth/Survival of Ovarian Carcinoma SKOV-3 Cells—To elucidate the functional role of TSG101 in ovarian cancer development, we disrupted the expression of TSG101 in SKOV-3 using a TSG101 siRNA duplex that has been successfully applied to specifically suppress the expression of endogenous TSG101 in several earlier studies (42–45). Suppression of TSG101 expression was confirmed by semiquantitative PCR and immunoblotting (Fig. 6, A and B). Initial observations showed no significant cellular effects in terms of rate of cell growth up to 72 h post-transfection of TSG101 siRNA. However, when the effect of TSG101 suppression on cell viability was carefully monitored by MTT assay as a function of time, SKOV-3 cells transfected with TSG101-specific siRNA started to decrease dramatically in number beginning 5 days post-transfection when compared with cells transfected with a scrambled control siRNA with the same GC content as the TSG101 siRNA (Fig. 6C). These results suggest that TSG101 is essential for the growth and survival of SKOV-3 cells.

In vivo tumor formation assay in nude mice was performed to determine whether TSG101 knockdown affects the tumorigenicity of SKOV-3 cells. SKOV-3 cells, 72 h post-transfection either with TSG101 or control siRNA duplex, were pairwise injected subcutaneously into the left or right flanks,

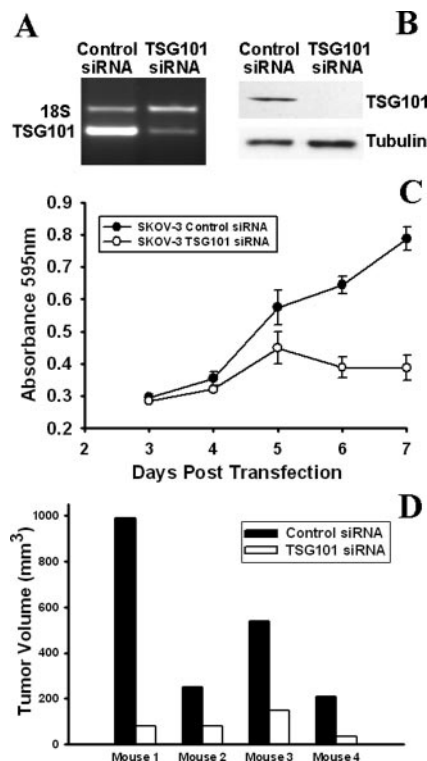


FIG. 6. Effects of gene silencing of TSG101 on SKOV-3 cell viability and tumorigenicity. SKOV-3 cells were transfected with TSG101 and control siRNAs as described under "Materials and Methods." RNA and protein were isolated as described. Levels of mRNA were determined by semiquantitative RT-PCR (A), and protein levels were determined by immunoblotting (B). Similar results were obtained from more than four independent experiments. C, siRNA-transfected SKOV-3 cells were plated at 2×10^3 cells/well in 96-well plates, and viability was monitored 3 days post-transfection over a 5-day period using MTT assay. Each data point represents an average of five independent readings \pm S.D. D, TSG101 siRNA knockdown reduces tumor growth of SKOV-3 cells in nude mice. Control (black bars) or TSG101 siRNA (open bars)-transfected SKOV-3 cells were injected into the right and left flanks (respectively) of 4–6-week-old BALB/c athymic nude mice on day 3 following siRNA transfection. Tumor volume was monitored over 4 weeks after which time tumors were excised and measured to determine final overall growth.

respectively, of the same BALB/c athymic nude mouse. Tumor growth was monitored for 6 weeks at which time the tumors were harvested and tumor volume was measured. In four mice tested, tumors formed from the SKOV-3 cells treated with TSG101 siRNA were significantly smaller than tumors formed from control siRNA cells (Fig. 6D). Due to the transient nature of the siRNA duplex, the actual effect of TSG101 gene silencing should be more prominent. Taken together, these results suggest that TSG101 is important for the growth, survival, and tumorigenicity of ovarian cancer cells.

TSG101 Knockdown Suppresses CITED2/HIF-1 α Expression and Activation—To determine the potential mechanism of TSG101 gene silencing-mediated inhibition of cell viability and tumorigenicity, we examined the expression of a panel of genes involved in cancer formation and cell survival. The

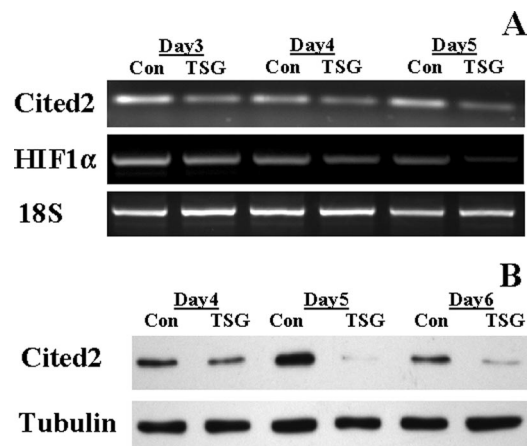


FIG. 7. Regulation of cellular levels of CITED2 and HIF-1 α by TSG101. A, levels of CITED2 and HIF-1 α mRNA were monitored by RT-PCR in SKOV-3 cells beginning 3 days post-transfection with either control (Con) or TSG101 (TSG) siRNA. B, cellular levels of CITED2 protein monitored by immunoblotting analysis using antibody specific for CITED2.

expression of two closely related transcriptional regulators, CITED2 and HIF-1 α , were found to be significantly down-regulated in SKOV-3 cells 3 days following TSG101 siRNA transfection (Fig. 7A). Both CITED2 and HIF-1 α have been implicated in regulating cell growth and survival. The decrease in CITED2 and HIF-1 α messenger occurred coincidentally with the decrease of SKOV-3 cell viability on the same time scale. Although the cellular protein levels of HIF-1 α were too low to be detected using Western blot analysis under normoxic conditions, the cellular levels of CITED2 were significantly reduced in SKOV-3 cells with TSG101 suppressed by siRNA (Fig. 7B).

To test the functional consequence of TSG101 knockdown-mediated down-regulation of CITED2/HIF-1 α , we examined HIF-1 α transcriptional activity using a HIF-1-inducible fluorescent reporter. This construct was created by splicing five copies of the HRE upstream of enhanced GFP, which provides a convenient method for monitoring HIF-1 activity levels by following GFP expression using fluorescence microscopy (46). As shown in Fig. 8A, fluorescent signal derived from GFP expression appeared significantly decreased in TSG101 knockdown cells 4 days post-transfection compared with controls. Immunoblotting analysis further confirmed a significantly decreased expression of GFP in TSG101 knockdown SKOV-3 cells (Fig. 8B). Taken together, these results indicate that TSG101 is an important regulator of HIF-1 α gene expression and transcriptional activation.

DISCUSSION

Collaboration among oncogenes and tumor suppressors represents a key mechanism of oncogenic transformation. Our recent study suggests that oncogenic RAS plays an important role in the epigenetic inactivation of opioid-binding protein/cell adhesion molecule-like gene, a recently identified tumor suppressor in human epithelial ovarian cancer (47). In

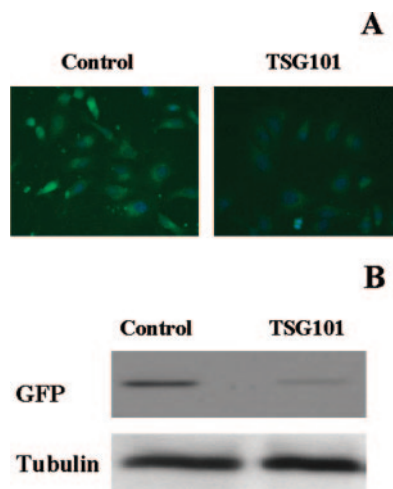


FIG. 8. Regulation of HIF-1 α -mediated transcriptional activation by TSG101. A, transcriptional activation as measured by expression of HRE-GFP reporter construct in SKOV-3 cells. SKOV-3 cells mounted on coverslips were transfected with HRE-GFP 3 days post-transfection with TSG101 or control siRNA. Two days following HRE-GFP transfection (5 days post-siRNA transfection), GFP fluorescence was determined using a fluorescence microscope equipped with a digital camera. B, SKOV-3 cells transfected with control or TSG101 siRNA and subsequently with HRE-GFP were lysed on day 5. HIF-1 α transcriptional activation was measured as a function of GFP protein levels probed using a GFP antibody (1:1000).

the present report, using a 2DE-based functional proteomics approach we identified TSG101 as a protein significantly altered post-transcriptionally following transformation of human ovarian surface epithelial cells with oncogenic *H-RAS* or *K-RAS*. To our knowledge, this is the first report linking RAS signaling and regulation of TSG101 protein levels. Previous studies show that the primary mechanism for TSG101 protein regulation occurs at the level of protein degradation (32), and TSG101 and MDM2 form an autoregulatory loop that modulates the cellular levels of both proteins (40). Our study demonstrates that oncogenic RAS, acting through the RAF/MEK/ERK signaling cascade as shown previously (48), up-regulates p14^{ARF}, which in turn suppresses cellular activity of HDM2 and consequently leads to the increase of cellular TSG101 protein levels in RAS-transformed cells. The clinical significance of the RAS-mediated TSG101 up-regulation is clearly demonstrated by the finding that the expression of TSG101 is increasingly positive in borderline tumors and low grade and high grade carcinomas, whereas normal ovarian epithelial cells show negative staining for TSG101. The ability to detect protein expression alterations in human ovarian carcinomas using a genetically defined cancer model and functional proteomics further validates the physiological relevance of this model and the value of the proteomics approach in cancer study.

To determine the significance of TSG101 up-regulation and the role that TSG101 may play in tumor formation and development in human ovarian cancer, we used siRNA to knock down TSG101 in the ovarian carcinoma cell line SKOV-3 with

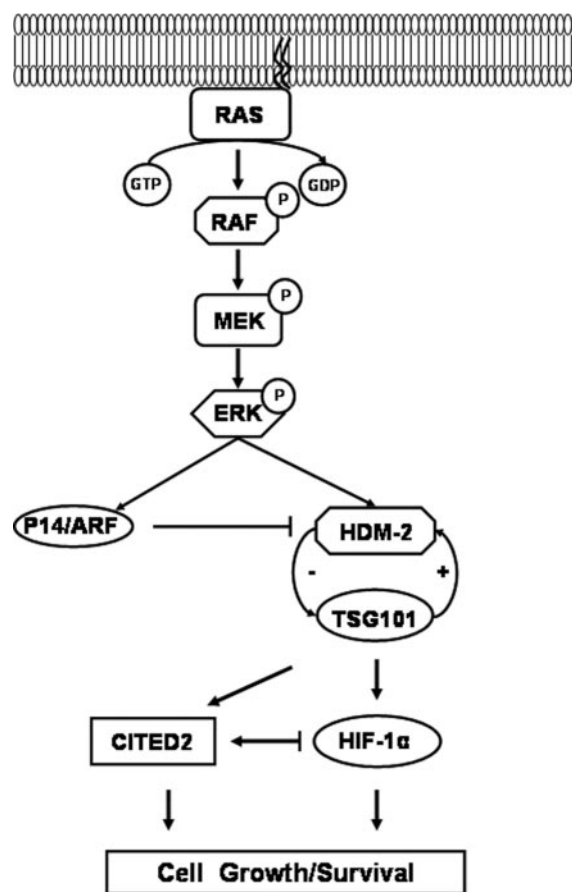


FIG. 9. Mechanism of RAS-mediated TSG101 regulation. Activation of the RAS/RAF/MEK/ERK signaling cascade leads to transcriptional induction of p14^{ARF} that suppresses cellular HDM2 activity (41). Inactivation of HDM2 leads to elevated cellular levels of TSG101 through a negative feedback loop (40). Increased TSG101 levels in ovarian cancer cells enhance CITED2/HIF-1 α expression and activation and subsequently promote cell growth and survival.

hyperactivated RAS signaling pathways similar to the engineered T29H cells (38). SKOV-3 cells exhibited significant growth inhibition and underwent apoptosis ~5 days following transfection with TSG101 siRNA. In addition, when injected into athymic nude mice, SKOV-3 cells with TSG101 silenced induced significantly smaller tumors *in vivo*, suggesting that TSG101 has a definitive prosurvival effect on this ovarian epithelial cancer cell line. These findings are in agreement with recent data pointing to a more growth-promoting rather than tumor-suppressive effect of TSG101 as proposed earlier (25, 27, 31) and suggest that oncogene RAS-mediated up-regulation of TSG101 is a positive factor for cell survival and tumor growth in ovarian cancer cells.

Suppression of TSG101 expression in SKOV-3 cells is accompanied by the reduction of CITED2 and HIF-1 α , two closely related transcriptional regulators that play important roles in the regulation of cell growth and survival. Gene knock-out of *Cited2* in mice resulted in embryonic lethality and premature senescence of the *Cited2*^{-/-} mouse embryonic

fibroblasts with increased expression of the cell proliferation inhibitors p16^{INK4a}, p19^{ARF}, and p15^{INK4b} (49, 50), whereas overexpression of CITED2 in Rat1 cells led to anchorage-independent growth in soft agar and tumor formation in nude mice (51). These observations suggest that CITED2 is essential for cell proliferation and survival. On the other hand, HIF-1 α controls the expression of more than 70 genes (52) and plays a critical role in cancer cell survival (53) and tumor migration and metastasis (54, 55). In addition to their individual roles in transcription regulation, HIF-1 α and CITED2 have also been shown to operate in a negative feedback loop through a common interaction with CBP/p300: HIF-1 α transcribes CITED2 during hypoxia, and accumulation of CITED2 inhibits HIF-1 α transactivation by blocking its interaction with CBP/p300 and restores normal oxygen homeostasis (56). Given the important roles that CITED2 and HIF-1 α play in cell proliferation and survival, the apparent growth-inhibitory and apoptotic effects of TSG101 gene silencing observed in the SKOV-3 cells may be partially mediated by the loss of CITED2/HIF-1 α expression.

In summary, we have demonstrated a novel mechanism of TSG101 regulation through the RAS signaling pathway. This regulatory mechanism appears to be post-translational in nature and likely involves p14^{ARF}/HDM2. From our studies and the observations of others, we conclude that RAS-mediated up-regulation of TSG101 provides progrowth/survival stimuli through the modulation of transcription regulators such as HIF-1 α and CITED2 (Fig. 9). This is consistent with the findings that oncogenic RAS-induced HIF-1 α via the RAF/MEK/MAPK pathway is important for RAS-mediated tumor promotion (57) and inhibition of RAS activation in glioblastoma leads to down-regulation of HIF-1 α and cell death (58). This connection among oncogenic RAS, TSG101, and HIF-1 α /CITED2 may play an important role for RAS-mediated oncogenic transformation as it has been shown that loss of HIF-1 α negatively affects tumor growth in oncogenic RAS-transformed cell lines (59). Finally our study demonstrates that TSG101 is overexpressed in ovarian carcinomas and may represent a potential target for future therapeutic intervention to inhibit growth and precipitate apoptosis of cancer cells.

Acknowledgments—We thank Dr. Yue Xiong and Yanping Zhang (University of North Carolina) for providing expression vector of HMD2 and Dr. Mark W. Dewhirst (Duke University Medical Center) for providing the HRE-driven GFP reporter construct.

* This work was supported in part by National Institute of Health Grant GM066170 and institutional startup funds (to X. C.). Help from the core facilities was supported by NIEHS, National Institutes of Health Center Grant ES06676. The costs of publication of this article were defrayed in part by the payment of page charges. This article must therefore be hereby marked “advertisement” in accordance with 18 U.S.C. Section 1734 solely to indicate this fact.

¶ Supported by American Cancer Society Research Scholar Grant RSG-04-028-01-CCE.

|| To whom correspondence should be addressed: Dept. of Pharmacology and Toxicology, The University of Texas Medical Branch,

301 University Blvd., Galveston, TX 77555-1031. Tel.: 409-772-9656; Fax: 409-772-9642; E-mail: xcheng@utmb.edu.

REFERENCES

- Singer, G., Oldt, R., III, Cohen, Y., Wang, B. G., Sidransky, D., Kurman, R. J., and Shih, I. (2003) Mutations in BRAF and KRAS characterize the development of low-grade ovarian serous carcinoma. *J. Natl. Cancer Inst.* **95**, 484–486
- Sieben, N. L., Macropoulos, P., Roemen, G. M., Kolkman-Uljee, S. M., Jan, F. G., Houmadi, R., Diss, T., Warren, B., Al Adnani, M., De Goeij, A. P., Krausz, T., and Flanagan, A. M. (2004) In ovarian neoplasms, BRAF, but not KRAS, mutations are restricted to low-grade serous tumours. *J. Pathol.* **202**, 336–340
- Varras, M. N., Sourvinos, G., Diakomanolis, E., Koumantakis, E., Flouris, G. A., Lekka-Katsouli, J., Michalakis, S., and Spandidos, D. A. (1999) Detection and clinical correlations of ras gene mutations in human ovarian tumors. *Oncology* **56**, 89–96
- Patton, S. E., Martin, M. L., Nelsen, L. L., Fang, X., Mills, G. B., Bast, R. C., Jr., and Ostrowski, M. C. (1998) Activation of the ras-mitogen-activated protein kinase pathway and phosphorylation of ets-2 at position threonine 72 in human ovarian cancer cell lines. *Cancer Res.* **58**, 2253–2259
- Berchuck, A., Kamel, A., Whitaker, R., Kerns, B., Olt, G., Kinney, R., Soper, J. T., Dodge, R., Clarke-Pearson, D. L., and Marks, P. (1990) Overexpression of HER-2/neu is associated with poor survival in advanced epithelial ovarian cancer. *Cancer Res.* **50**, 4087–4091
- Gemignani, M. L., Schlaerth, A. C., Bogomolny, F., Barakat, R. R., Lin, O., Soslow, R., Venkatraman, E., and Boyd, J. (2003) Role of KRAS and BRAF gene mutations in mucinous ovarian carcinoma. *Gynecol. Oncol.* **90**, 378–381
- Marshall, C. J. (1995) Specificity of receptor tyrosine kinase signaling: transient versus sustained extracellular signal-regulated kinase activation. *Cell* **80**, 179–185
- Berchuck, A., and Carney, M. (1997) Human ovarian cancer of the surface epithelium. *Biochem. Pharmacol.* **54**, 541–544
- Vavvas, D., Li, X., Avruch, J., and Zhang, X. F. (1998) Identification of Nore1 as a potential Ras effector. *J. Biol. Chem.* **273**, 5439–5442
- Wadari, Y., Kariya, K., Shibatohe, M., Liao, Y., Hu, C. D., Goshima, M., Tamada, M., Kikuchi, A., and Kataoka, T. (1998) Identification of Ce-RAF-6, a novel *Caenorhabditis elegans* protein, as a putative Ras effector. *Gene (Amst.)* **224**, 53–58
- Shibatohe, M., Kariya, K., Liao, Y., Hu, C. D., Wadari, Y., Goshima, M., Shima, F., and Kataoka, T. (1998) Identification of PLC210, a *Caenorhabditis elegans* phospholipase C, as a putative effector of Ras. *J. Biol. Chem.* **273**, 6218–6222
- Khosravi-Far, R., White, M. A., Westwick, J. K., Solski, P. A., Chrzanowska-Wodnicka, M., Van Aelst, L., Wigler, M. H., and Der, C. J. (1996) Oncogenic Ras activation of Raf/mitogen-activated protein kinase-independent pathways is sufficient to cause tumorigenic transformation. *Mol. Cell. Biol.* **16**, 3923–3933
- Kauffmann-Zeh, A., Rodriguez-Viciano, P., Ulrich, E., Gilbert, C., Coffey, P., Downward, J., and Evan, G. (1997) Suppression of c-Myc-induced apoptosis by Ras signalling through PI(3)K and PKB. *Nature* **385**, 544–548
- Feig, L. A., Urano, T., and Cantor, S. (1996) Evidence for a Ras/Ral signaling cascade. *Trends Biochem. Sci.* **21**, 438–441
- Li, L., and Cohen, S. N. (1996) Tsg101: a novel tumor susceptibility gene isolated by controlled homozygous functional knockout of allelic loci in mammalian cells. *Cell* **85**, 319–329
- Li, L., Li, X., Francke, U., and Cohen, S. N. (1997) The TSG101 tumor susceptibility gene is located in chromosome 11 band p15 and is mutated in human breast cancer. *Cell* **88**, 143–154
- Li, L., Francke, U., and Cohen, S. N. (1998) Retraction. The TSG101 tumor susceptibility gene is located in chromosome 11 band p15 and is mutated in human breast cancer. *Cell* **93**, following 660
- Lee, M. P., and Feinberg, A. P. (1997) Aberrant splicing but not mutations of TSG101 in human breast cancer. *Cancer Res.* **57**, 3131–3134
- Gayther, S. A., Barski, P., Batley, S. J., Li, L., de Foy, K. A., Cohen, S. N., Ponder, B. A., and Caldas, C. (1997) Aberrant splicing of the TSG101 and FHIT genes occurs frequently in multiple malignancies and in normal tissues and mimics alterations previously described in tumours. *Oncogene* **15**, 2119–2126
- Wang, Q., Driouch, K., Courtois, S., Champeme, M. H., Bieche, I., Treilleux,

- I., Briffod, M., Rimokh, R., Magaud, J. P., Curmi, P., Lidereau, R., and Puisieux, A. (1998) Low frequency of TSG101/CC2 gene alterations in invasive human breast cancers. *Oncogene* **16**, 677–679
21. Steiner, P., Barnes, D. M., Harris, W. H., and Weinberg, R. A. (1997) Absence of rearrangements in the tumour susceptibility gene TSG101 in human breast cancer. *Nat. Genet.* **16**, 332–333
 22. Sun, Z., Pan, J., Bublej, G., and Balk, S. P. (1997) Frequent abnormalities of TSG101 transcripts in human prostate cancer. *Oncogene* **15**, 3121–3125
 23. Wagner, K. U., Dierisseau, P., Rucker, E. B., III, Robinson, G. W., and Hennighausen, L. (1998) Genomic architecture and transcriptional activation of the mouse and human tumor susceptibility gene TSG101: common types of shorter transcripts are true alternative splice variants. *Oncogene* **17**, 2761–2770
 24. Ruland, J., Sirard, C., Elia, A., MacPherson, D., Wakeham, A., Li, L., de la Pompa, J. L., Cohen, S. N., and Mak, T. W. (2001) p53 accumulation, defective cell proliferation, and early embryonic lethality in mice lacking *tsg101*. *Proc. Natl. Acad. Sci. U. S. A.* **98**, 1859–1864
 25. Krempler, A., Henry, M. D., Triplett, A. A., and Wagner, K. U. (2002) Targeted deletion of the *Tsg101* gene results in cell cycle arrest at G1/S and p53-independent cell death. *J. Biol. Chem.* **277**, 43216–43223
 26. Wagner, K. U., Krempler, A., Qi, Y., Park, K., Henry, M. D., Triplett, A. A., Riedlinger, G., Rucker, E. B., III, and Hennighausen, L. (2003) *Tsg101* is essential for cell growth, proliferation, and cell survival of embryonic and adult tissues. *Mol. Cell. Biol.* **23**, 150–162
 27. Carstens, M. J., Krempler, A., Triplett, A. A., Van Lohuizen, M., and Wagner, K. U. (2004) Cell cycle arrest and cell death are controlled by p53-dependent and p53-independent mechanisms in *Tsg101*-deficient cells. *J. Biol. Chem.* **279**, 35984–35994
 28. Bennett, N. A., Pattillo, R. A., Lin, R. S., Hsieh, C. Y., Murphy, T., and Lyn, D. (2001) TSG101 expression in gynecological tumors: relationship to cyclin D1, cyclin E, p53 and p16 proteins. *Cell. Mol. Biol. (Noisy-le-grand)* **47**, 1187–1193
 29. Liu, R. T., Huang, C. C., You, H. L., Chou, F. F., Hu, C. C., Chao, F. P., Chen, C. M., and Cheng, J. T. (2002) Overexpression of tumor susceptibility gene TSG101 in human papillary thyroid carcinomas. *Oncogene* **21**, 4830–4837
 30. Koon, N., Schneider-Stock, R., Sarlomo-Rikala, M., Lasota, J., Smolkin, M., Petroni, G., Zaika, A., Boltze, C., Meyer, F., Andersson, L., Knuutila, S., Miettinen, M., and El Rifai, W. (2004) Molecular targets for tumour progression in gastrointestinal stromal tumours. *Gut* **53**, 235–240
 31. Zhu, G., Gilchrist, R., Borley, N., Chng, H. W., Morgan, M., Marshall, J. F., Camplejohn, R. S., Muir, G. H., and Hart, I. R. (2004) Reduction of TSG101 protein has a negative impact on tumor cell growth. *Int. J. Cancer* **109**, 541–547
 32. Feng, G. H., Lih, C. J., and Cohen, S. N. (2000) TSG101 protein steady-state level is regulated posttranslationally by an evolutionarily conserved COOH-terminal sequence. *Cancer Res.* **60**, 1736–1741
 33. Liu, J., Yang, G., Thompson-Lanza, J. A., Glassman, A., Hayes, K., Patterson, A., Marquez, R. T., Auersperg, N., Yu, Y., Hahn, W. C., Mills, G. B., and Bast, R. C., Jr. (2004) A genetically defined model for human ovarian cancer. *Cancer Res.* **64**, 1655–1663
 34. Young, T. W., Mei, F. C., Yang, G., Thompson-Lanza, J. A., Liu, J., and Cheng, X. (2004) Activation of antioxidant pathways in ras-mediated oncogenic transformation of human surface ovarian epithelial cells revealed by functional proteomics and mass spectrometry. *Cancer Res.* **64**, 4577–4584
 35. Young, T., Mei, F., Liu, J., Bast, R. C., Jr., Kurosky, A., and Cheng, X. (2005) Proteomics analysis of H-RAS-mediated oncogenic transformation in a genetically defined human ovarian cancer model. *Oncogene* **24**, 6174–6184
 36. Blum, H., Beier, H., and Gross, H. L. (1987) Improved silver staining of plant proteins, RNA and DNA in polyacrylamide gels. *Electrophoresis* **8**, 93–99
 37. Shevchenko, A., Wilm, M., Vorm, O., and Mann, M. (1996) Mass spectrometric sequencing of proteins silver-stained polyacrylamide gels. *Anal. Chem.* **68**, 850–858
 38. Yang, G., Thompson, J. A., Fang, B., and Liu, J. (2003) Silencing of H-ras gene expression by retrovirus-mediated siRNA decreases transformation efficiency and tumor growth in a model of human ovarian cancer. *Oncogene* **22**, 5694–5701
 39. Hancock, J. F., Paterson, H., and Marshall, C. J. (1990) A polybasic domain or palmitoylation is required in addition to the CAAX motif to localize p21ras to the plasma membrane. *Cell* **63**, 133–139
 40. Li, L., Liao, J., Ruland, J., Mak, T. W., and Cohen, S. N. (2001) A TSG101/MDM2 regulatory loop modulates MDM2 degradation and MDM2/p53 feedback control. *Proc. Natl. Acad. Sci. U. S. A.* **98**, 1619–1624
 41. Ries, S., Biederer, C., Woods, D., Shifman, O., Shirasawa, S., Sasazuki, T., McMahan, M., Oren, M., and McCormick, F. (2000) Opposing effects of Ras on p53: transcriptional activation of *mdm2* and induction of p19ARF. *Cell* **103**, 321–330
 42. Garrus, J. E., von Schwedler, U. K., Pornillos, O. W., Morham, S. G., Zavitz, K. H., Wang, H. E., Wettstein, D. A., Stray, K. M., Cote, M., Rich, R. L., Myszka, D. G., and Sundquist, W. I. (2001) *Tsg101* and the vacuolar protein sorting pathway are essential for HIV-1 budding. *Cell* **107**, 55–65
 43. Hewitt, E. W., Duncan, L., Mufti, D., Baker, J., Stevenson, P. G., and Lehner, P. J. (2002) Ubiquitylation of MHC class I by the K3 viral protein signals internalization and TSG101-dependent degradation. *EMBO J.* **21**, 2418–2429
 44. Amit, I., Yakir, L., Katz, M., Zwang, Y., Marmor, M. D., Citri, A., Shtiegman, K., Alroy, I., Tuvia, S., Reiss, Y., Roubini, E., Cohen, M., Wides, R., Bacharach, E., Schubert, U., and Yarden, Y. (2004) Tal, a Tsg101-specific E3 ubiquitin ligase, regulates receptor endocytosis and retrovirus budding. *Genes Dev.* **18**, 1737–1752
 45. Ismaili, N., Blind, R., and Garabedian, M. J. (2005) Stabilization of the unliganded glucocorticoid receptor by TSG101. *J. Biol. Chem.* **280**, 11120–11126
 46. Moeller, B. J., Cao, Y., Li, C. Y., and Dewhirst, M. W. (2004) Radiation activates HIF-1 to regulate vascular radiosensitivity in tumors: role of reoxygenation, free radicals, and stress granules. *Cancer Cell* **5**, 429–441
 47. Mei, F. C., Young, T. W., Liu, J., and Cheng, X. (2006) RAS-mediated epigenetic inactivation of OPCML in oncogenic transformation of human ovarian surface epithelial cells. *FASEB J.* **20**, 497–499
 48. Palmero, I., Pantoja, C., and Serrano, M. (1998) p19ARF links the tumour suppressor p53 to Ras. *Nature* **395**, 125–126
 49. Yin, Z., Haynie, J., Yang, X., Han, B., Kiatchoosakun, S., Restivo, J., Yuan, S., Prabhakar, N. R., Herrup, K., Conlon, R. A., Hoyt, B. D., Watanabe, M., and Yang, Y. C. (2002) The essential role of Cited2, a negative regulator for HIF-1 α , in heart development and neurulation. *Proc. Natl. Acad. Sci. U. S. A.* **99**, 10488–10493
 50. Kranc, K. R., Bamforth, S. D., Braganca, J., Norbury, C., Van Lohuizen, M., and Bhattacharya, S. (2003) Transcriptional coactivator Cited2 induces Bmi1 and Mel18 and controls fibroblast proliferation via Ink4a/ARF. *Mol. Cell. Biol.* **23**, 7658–7666
 51. Sun, H. B., Zhu, Y. X., Yin, T., Sledge, G., and Yang, Y. C. (1998) MRG1, the product of a melanocyte-specific gene related gene, is a cytokine-inducible transcription factor with transformation activity. *Proc. Natl. Acad. Sci. U. S. A.* **95**, 13555–13560
 52. Mazure, N. M., Brahimi-Horn, M. C., Berta, M. A., Benizri, E., Bilton, R. L., Dayan, F., Ginouves, A., Berra, E., and Pouyssegur, J. (2004) HIF-1: master and commander of the hypoxic world. A pharmacological approach to its regulation by siRNAs. *Biochem. Pharmacol.* **68**, 971–980
 53. Semenza, G. L. (2003) Targeting HIF-1 for cancer therapy. *Nat. Rev. Cancer* **3**, 721–732
 54. Pennacchietti, S., Michieli, P., Galluzzo, M., Mazzone, M., Giordano, S., and Comoglio, P. M. (2003) Hypoxia promotes invasive growth by transcriptional activation of the met protooncogene. *Cancer Cell* **3**, 347–361
 55. Yang, Z. F., Poon, R. T., To, J., Ho, D. W., and Fan, S. T. (2004) The potential role of hypoxia inducible factor 1 α in tumor progression after hypoxia and chemotherapy in hepatocellular carcinoma. *Cancer Res.* **64**, 5496–5503
 56. Tien, E. S., Davis, J. W., and Vanden Heuvel, J. P. (2004) Identification of the CREB-binding protein/p300-interacting protein CITED2 as a peroxisome proliferator-activated receptor α coregulator. *J. Biol. Chem.* **279**, 24053–24063
 57. Lim, J. H., Lee, E. S., You, H. J., Lee, J. W., Park, J. W., and Chun, Y. S. (2004) Ras-dependent induction of HIF-1 α 785 via the Raf/MEK/ERK pathway: a novel mechanism of Ras-mediated tumor promotion. *Oncogene* **23**, 9427–9431
 58. Blum, R., Jacob-Hirsch, J., Amariglio, N., Rechavi, G., and Kloog, Y. (2005) Ras inhibition in glioblastoma down-regulates hypoxia-inducible factor-1 α , causing glycolysis shutdown and cell death. *Cancer Res.* **65**, 999–1006
 59. Ryan, H. E., Poloni, M., McNulty, W., Elson, D., Gassmann, M., Arbeit, J. M., and Johnson, R. S. (2000) Hypoxia-inducible factor-1 α is a positive factor in solid tumor growth. *Cancer Res.* **60**, 4010–4015